Available online at www.sciencedirect.com

ScienceDirect

Energy Procedia 129 (2017) 875–882

Energy Procedia

www.elsevier.com/locate/procedia

IV International Seminar on ORC Power Systems, ORC2017
13-15 September 2017, Milano, Italy

Experimental Investigation of the Operating Point of a 1-kW ORC System

Chinedu K. Unamba[a], Martin White[a], Paul Sapin[a], James Freeman[a], Steven Lecompte[b], Oyeniyi A. Oyewunmi[a] and Christos N. Markides[a,*]

[a] *Clean Energy Processes (CEP) Laboratory, Department of Chemical Engineering, Imperial College London, London SW7 2AZ, UK*
[b] *Department of Flow, Heat and Combustion Mechanics, Ghent University, Sint-Pietersnieuwstraat 41, Belgium*

Abstract

The organic Rankine cycle (ORC) is a promising technology for the conversion of waste heat from industrial processes as well as heat from renewable sources. Many efforts have been channeled towards maximizing the thermodynamic potential of ORC systems through the selection of working fluids and the optimal choice of operating parameters with the aim of improving overall system designs, and the selection and further development of key components. Nevertheless, experimental work has typically lagged behind modelling efforts. In this paper, we present results from tests on a small-scale (1 kWel) ORC engine consisting of a rotary-vane pump, a brazed-plate evaporator and a brazed-plate condenser, a scroll expander with a built-in volume ratio of 3.5, and using R245fa as the working fluid. An electric oil-heater acted as the heat source, providing hot oil at temperatures in the range 120-140 °C. The frequency of the expander was not imposed by an inverter or the electricity grid but depended directly on the attached generator load; both the electrical load on the generator and the pump rotational speed were varied in order to investigate the performance of the system. Based on the generated data, this paper explores the relationship between the operating conditions of the ORC engine and changes in the heat-source temperature, pump and expander speeds leading to working fluid flow rates between 0.0088 kg/s and 0.0337 kg/s, from which performance maps are derived. The experimental data is, in turn, used to assess the performance of both the individual components and of the system, with the help of an exergy analysis. In particular, the exergy analysis indicates that the expander accounts for the second highest loss in the system. Analysis of the results suggests that increased heat-source temperatures, working-fluid flow rates, higher pressure ratios and larger generator loads improve the overall cycle efficiency. Specifically, a 46% increase in pressure ratio from 2.4 to 4.4 allowed a 3-fold electrical power output increase from 180 W to 550 W, and an increase in the thermal efficiency of the ORC engine from 1 to 4%. Beyond reporting on important lessons learned in improving the performance of the system under consideration, comparisons will be shown for making proper choices with respect to the interplay between heat-source temperature, generator load, and pump speed in an ORC system.

Peer-review under responsibility of the scientific committee of the IV International Seminar on ORC Power Systems.

* Corresponding author. Tel.: +44 (0)20 759 41601. *E-mail address:* c.markides@imperial.ac.uk; Web page: www.imperial.ac.uk/cep

1876-6102
Peer-review under responsibility of the scientific committee of the IV International Seminar on ORC Power Systems.
10.1016/j.egypro.2017.09.211

Keywords: exergy analysis; experimental testbed; off design; organic Rankine cycle; part load.

Nomenclature						
$\dot{E}$	W	Exergy transfer/flow rate	**Greek**		2	Evaporator inlet, pump outlet
$\dot{E}_i^{\mathrm{a}}$	W	Available exergy	η_{e}, η_{p}	Expander/pump efficiency	3	Expander inlet, evaporator outlet
$\dot{E}_i^{\mathrm{u}}$	W	Used exergy	η_{ex}	Exergy efficiency	4	Condenser inlet, expander outlet
$\dot{E}_{\mathrm{Q}}$	W	Exergy transfer by heat	η_{th}	Thermal efficiency	cd	Condenser
h	J/kg	Specific enthalpy			e	Expander
$\dot{I}$	W	Irreversible exergy loss rate	**Abbreviations**		ev	Evaporator
i	-	Component	ORC	Organic Rankine cycle	ex	Exergy
$\dot{m}$	kg/s	Mass flow rate			in	Into component
P	Pa, bar	Pressure	**Superscripts**		o	Dead state
$\dot{Q}$	W	Heat transfer/flow rate	a	Available	out	Out of component
r_{p}	-	Pressure ratio	u	Used	p	Pump
s	J/kg K	Specific entropy			th	Thermal
T	K, °C	Temperature	**Subscripts**		x	Shaft
$\dot{W}$	W	Power	1	Pump inlet, condenser outlet		

1. Introduction

Interest in ORC technology stems from the desire to produce electricity from renewable or low-/medium-grade waste heat, and has grown considerably over the past few decades [1,2]. In the context of waste heat, the heat source is usually considered "free" in that it is being rejected from other processes. ORC technology can help curb our current dependence on fossil fuels, while reducing harmful emissions and pollution, promoting independence and conserving resources [3,4]. In particular, a broad variety of processes can be found in industrial plants rejecting a significant amount of thermal energy in the form of combustion products into the atmosphere over a range of scales and temperatures [5]. Studies have found that about 60% of industrial energy input is typically wasted [6].

In developing nations, like most African countries, one of the limiting factors of economic and technological progress is the availability of electricity, while at the same time there exists thousands of manufacturing plants whose rejected thermal energy can be converted to electricity. ORC technology can be used to convert this thermal-energy resource, electrifying homes, business and industrial facilities. The need to understand the potential (suitable system architectures and designs, optimal performance and operation) of ORCs systems in this context is imperative.

Many studies have been performed based on combining first-law (energy) and second-law (exergy) thermodynamic cycle analyses, e.g., see Ref. [7], aimed at understanding the performance characteristics of ORC systems. In one such study, Baral et al. [8] investigated the role of the heat-source temperature, pressure ratio and expander load in determining the ORC system thermal efficiency, component efficiencies and system power output. At different stages of ORC system design, choices have to be made concerning several operating parameters and component selection, namely the choice of expander, pump and refrigerant. In addition, the properties of the working fluid have a great influence on the overall system performance; for example, some working fluids may require a large superheat which could be detrimental to cycle efficiency [9-10]. In addition to these selection criteria, component selection is also important, e.g., volumetric expanders are usually preferred at smaller-scale and lower-temperature applications, where this study focuses due to their low-speed and two-phase fluid tolerance, as well as their low cost [11].

This paper aims to investigate how the adjustment of important system parameters can affect the operation and performance of a practical ORC system, while generating and making data available in the literature that can be used for the development and validation of complementary modelling efforts. Changes were made to the heat-source temperature, system pressure ratio, working-fluid flow rate, electrical generator load, and system performance maps have been captured. It is noteworthy that a source of confusion and misunderstanding lies in the definition of various first-law efficiency measures [12]. Evaluating the ORC system performance and identifying areas for improvement can also be attempted by exergy approaches. For example, previous studies have shown that the expander has the second largest exergy destruction after the evaporator [13]. Therefore, in addition to analysing the performance using first law arguments, an exergy analysis of each major system component is also performed based on results from the experimental tests.

2. System Description

Experiments were performed to determine the performance of a 1-kW ORC testbed system over a range of operating conditions. The aim was to investigate how the performance of the scroll expander and the pump, as well as the overall thermal efficiency of the cycle and exergetic performance of key components were affected by changes to important operational parameters, including the heat-source temperature, pump speed, pressure ratio and generator load.

The ORC system comprises a rotary vane pump (TMFRSS051A), a brazed-plate evaporator, a 1-kWel semi hermetic scroll expander (E15H022A-SH) connected to an A/C generator through a magnetic coupling and a brazed-plate condenser (CB80-30H-F). In the experiments, the working fluid (R245fa) was compressed by the pump and entered the evaporator where it was superheated by 10 to 62 °C. A 20-kWth electric oil heater served as the heat-source, heating a flow of oil (thermoil) that simulated a liquid-phase waste-heat source stream to a temperature set to either 120 °C, 130 °C or 140 °C, and a flow rate of 1.4 L/s. The condenser was water cooled, with water entering and leaving the condenser at conditions maintained at 19 and 21 °C, respectively, at a flow rate of 22 L/min.

The nominal electrical load connected to the generator, denoted as “full load”, consisted of two 100 W light bulbs and two 100 Ω heat-dissipating resistors connected in four parallel circuits. Under “partial load” condition, the two resistor circuits were disconnected. For a given test condition, the pump speed was varied from 1100 RPM to 3500 RPM, allowing variations to working-fluid flow rate as well as to the pressure ratio.

The system was allowed to reach steady-state conditions before values were recorded. The pressure and the temperature values at the inlet and exit of each component were measured via pressure transducers and thermocouples. The speed of the pump was varied from 1100 RPM to 3600 RPM (this caused a change in mass flow rate and increase in pump outlet pressure) at a particular heat source temperature and different expander torque. The working-fluid mass-flow rate was measured using an ultrasonic flow meter at the pump inlet, while the expander-generator electrical power output and ORC pump electrical input power were measured using digital power meters. System temperatures were measured using T-type thermocouples with a stated accuracy of ±1 °C, and system pressures were measured using analogue pressure transducers with a full-scale accuracy of ±0.25%. A schematic diagram of the ORC testing facility including measurement locations is shown in Fig. 1.

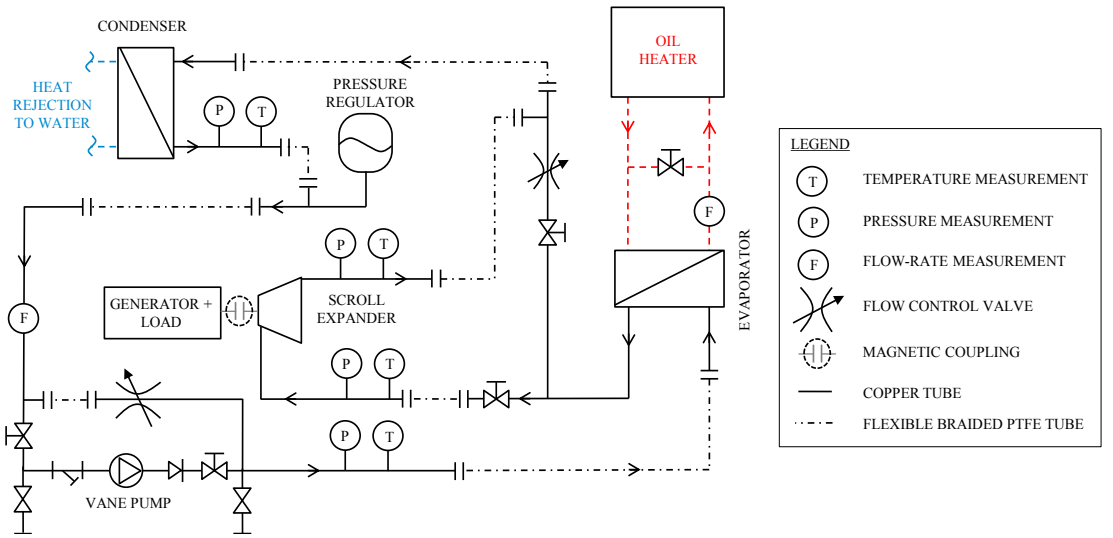

Figure 1: Schematic of the ORC testing facility with salient measurement points and key cycle states indicated.

3. ORC Performance and Error Analysis

In evaluating the results from the ORC unit, the following assumptions were made:

- The system operates in steady state;
- Pressure drops across the condenser, evaporator and along the connecting pipes can be neglected.

Hence, based on the pump power consumption, $\dot{W}_{\mathrm{p}}$, measured by an energy meter, the pump efficiency, η_{p}, is defined as:

$$\eta_{\mathrm{p}} = \frac{\dot{m}(h_{2s}-h_1)}{\dot{W}_{\mathrm{p}}} \tag{1}$$

while the power generated by the expander, $\dot{W}_{\mathrm{e}}$, was measured from the power meter connected to the expander and the expander isentropic efficiency, η_{e}, calculated from:

$$\eta_{\mathrm{e}} = \frac{\dot{W}_{\mathrm{e}}}{\dot{m}(h_3-h_{4s})} \tag{2}$$

The heat transferred to the working fluid in the evaporator, $\dot{Q}_{\mathrm{ev}}$, and rejected to the heat sink in the condenser, $\dot{Q}_{\mathrm{cd}}$, are:

$$\dot{Q}_{\mathrm{ev}} = \dot{m}(h_3 - h_2) \tag{3}$$
$$\dot{Q}_{\mathrm{cd}} = \dot{m}(h_4 - h_1) \tag{4}$$

and finally, the thermal efficiency of the ORC unit is given by:

$$\eta_{\mathrm{th}} = \frac{\dot{W}_{\mathrm{e}}-\dot{W}_{\mathrm{p}}}{\dot{Q}_{\mathrm{ev}}} \tag{5}$$

An error analysis on the performance parameters defined above has been performed, yet not detailed in the present paper. The results are indicated as error bars in the figures in Section 5 (Figures 2 to 5).

4. Exergy Analysis

Exergy represents the potential to perform useful work and, unlike energy, is destroyed during irreversible (*i.e.*, to some extent in all practical) processes due to thermodynamic losses, *e.g.*, due to heat losses to the environment [14]. For the present exergy analysis, the following assumptions were made:

- Potential and kinetic energy changes were neglected;
- The dead state temperature and pressure were 19 °C and atmospheric pressure, respectively.

Given these assumptions, the mass, energy and exergy balance equations for a control volume at steady state are:

$$\sum \dot{m}_{\mathrm{in}} = \sum \dot{m}_{\mathrm{out}} \tag{6}$$
$$\dot{Q} - \dot{W}_{\mathrm{x}} = \sum \dot{m}_{\mathrm{out}} h_{\mathrm{out}} - \sum \dot{m}_{\mathrm{in}} h_{\mathrm{in}} \tag{7}$$
$$\dot{E}_{\mathrm{Q}} - \dot{W}_{\mathrm{x}} = \sum \dot{E}_{\mathrm{out}} - \sum \dot{E}_{\mathrm{in}} + \dot{I} \tag{8}$$

where $\dot{W}_{\mathrm{x}}$ is the shaft work, $\dot{E}_{\mathrm{Q}}$ is the net exergy transfer by heat transfer $\dot{Q}$ at temperature T given by:

$$\dot{E}_{\mathrm{Q}} = \sum \left(1 - \frac{T_0}{T}\right) \dot{Q} \tag{9}$$

and the exergy flow rate in fluid stream *i* is given by:

$$\dot{E}_i = \dot{m}[h - h_{\mathrm{o}} - T_{\mathrm{o}}(s - s_{\mathrm{o}})] \tag{10}$$

where T_{o} and s_{o} are the dead state temperature and entropy respectively.

In the present work, all terms in Eq. (8) are known from direct measurements, except from the internal exergy losses associated with irreversibility, $\dot{I}$. Therefore, in component *i*, this term can be evaluated from re-arranging this expression:

$$\dot{I}_i = \dot{E}_{\mathrm{in},i} - \dot{E}_{\mathrm{out},i} + \dot{E}_{\mathrm{Q},i} - \dot{W}_{\mathrm{x},i} \tag{11}$$

The exergy efficiency of component *i* is the ratio of the used exergy in that component to the available exergy at the same component, and here we use the definitions as provided in Ref. [13]:

$$\eta_{\mathrm{ex},i} = \frac{\dot{E}_i^{\mathrm{u}}}{\dot{E}_i^{\mathrm{a}}} \tag{12}$$

Finally, the overall ORC system exergy efficiency is given by [13]:

$$\eta_{\mathrm{ex}} = \frac{\sum \dot{E}_i^{\mathrm{u}}}{\sum \dot{E}_i^{\mathrm{a}}} \tag{13}$$

By means of clarification, the available exergy is defined here the amount of exergy provided to a component by a source (*e.g.*, the shaft input work for a pump or compressor, or the fluid enthalpy drop through an expander), while the used exergy is the amount of available exergy converted into a useful output (*e.g.*, the fluid enthalpy rise delivered by a pump or compressor, or the shaft work output from an expander) [13].

5. Results and Discussion

The analyses presented in Sections 3 and 4 have been used to evaluate the performance of the ORC system presented in Section 2. Six operating-condition cases have been evaluated, covering the three different heat-source temperatures mentioned above (120 °C, 130 °C, and 140 °C) at both full and part generator load operation.

In Figure 2(a) it can be seen that as the pump speed increases, the pressure ratio increases as expected, resulting in an increase in the working-fluid mass flow rate. Hence, the electrical power required by the pump at these higher pressure ratios, or pump speeds, increases as shown in Figure 2(b). There is no significant change in the pumping power requirement with a change in the heat-source temperature, or in the generator load.

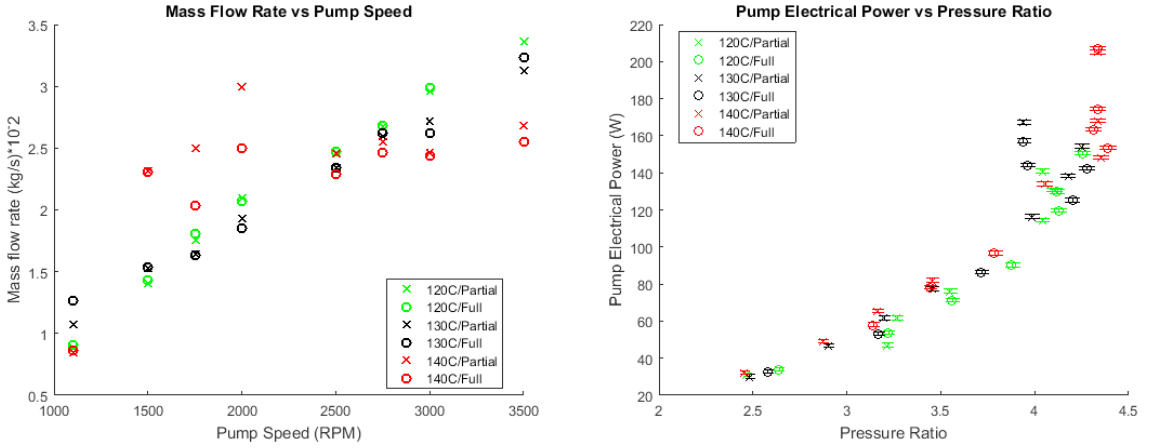

(a) (b)

Figure 2: (a) Effect of pump speed, heat-source temperature and expander/generator load on mass flow rate. (b) Effect of pressure ratio, heat-source temperature and expander/generator load on pump electrical power.

Corresponding performance results relating to the operation of the expander are shown in Figure 3. The electrical power generated by the expander-generator combination increases as the pressure ratio increases, as expected. When the full generator load is engaged, the system is able to generate a maximum electrical output of 600 W at a pressure ratio of 4.3 (corresponding to 60% of the stated nominal expander-generator output). For the partial-load configuration, a maximum electrical power output of 200 W is achieved, again at a pressure ratio of 4.3. At full generator load, an increasing heat-source temperature results in a slightly increased expander power output and an increase in the pressure ratio measured across the expander. At partial generator load, increasing the heat source temperature showed little or no advantage in terms of increasing electrical power output, particularly at higher pressure ratios.

The isentropic efficiency of the expander attains a maximum (around ~80%) at pressure ratios between 3.2 and 3.8 at full generator load, as shown in Figure 3(b). Interestingly, the intermediate heat-source temperature appears to give the maximum overall isentropic-efficiency value, at a pressure ratio of 3.7, which this is considered to be a suitable pressure ratio across the expander. Nevertheless, this observation must be seen in the context of the relative errors in the measurement of the efficiency indicated by the bars in Figure 3(b), which are of the order of ±10%.

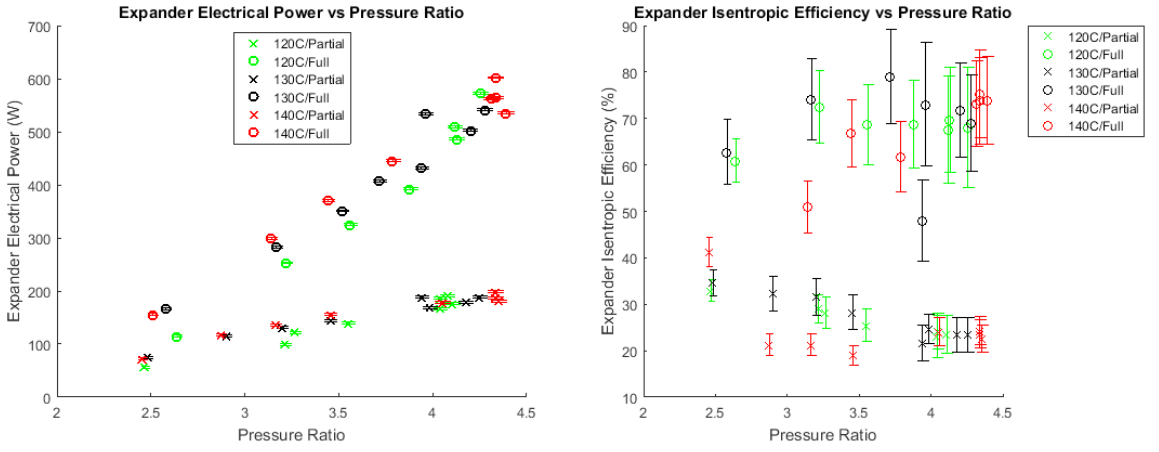

(a) (b)

Figure 3: (a) Effect of pressure ratio, heat-source temperature and generator load on expander electrical power. (b): Effect of pressure ratio, heat-source temperature and generator load on expander isentropic efficiency.

The cycle thermal efficiency is plotted in Figure 4, and this increases generally with pressure ratio at both part and full generator load. The overall trend is a result of the expander power output increasing, shown in Fig. 3a. At full generator load, the cycle efficiency increases with pressure ratio also because the generator load can absorb more of the power generated by the expander-generator compared to the part-load conditions, reaching a maximum of ~6% at a pressure ratio of 3.6. At part generator load, the thermal efficiency shows a slight decrease as the pressure ratio increases beyond 3.1.

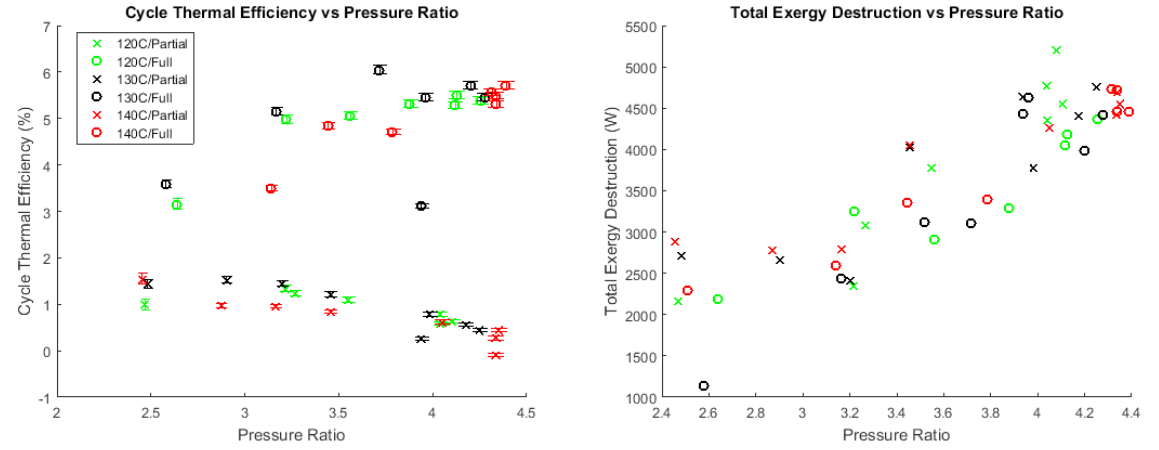

(a) (b)

Figure 4: (a) Effect of pressure ratio, heat-source temperature and generator load on cycle thermal efficiency. (b) Effect of pressure ratio, heat-source temperature and generator load on total exergy destruction.

The exergy analysis was performed on the four main system components and the total exergy destruction is plotted in Figure 5. It is observed that the exergy destruction increased at higher pressure ratios but was insensitive to the heat-source temperature at which the tests were performed and also to the generator load used on the expender-generator.

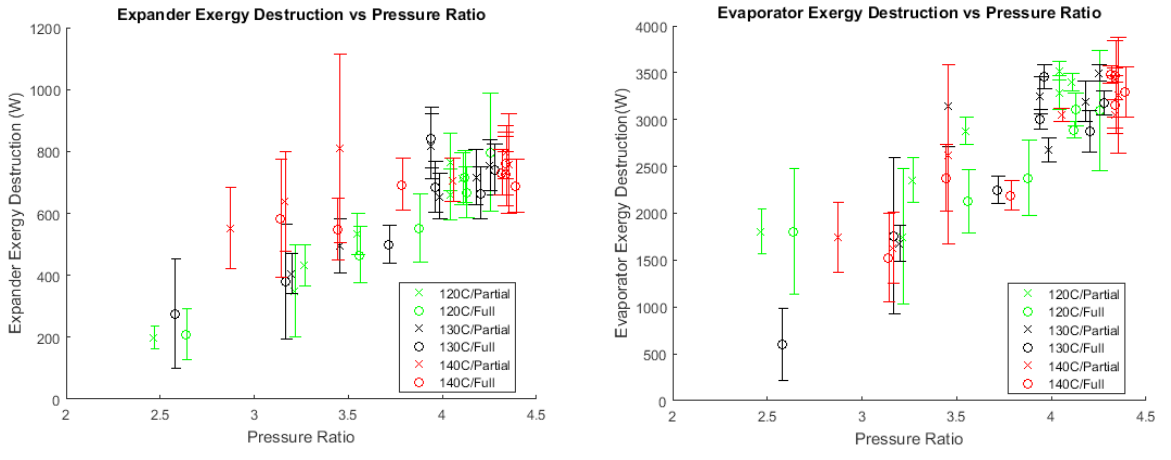

Figure 5: (a) Effect of pressure ratio, heat-source temperature and generator load on expander exergy destruction. (b) Effect of pressure ratio, heat-source temperature and generator load on evaporator exergy destruction.

A further analysis of the exergy breakdown within the system (normalized by the total) at part and full generator load are shown in Fig. 6a and 6b, respectively. The results have been plotted for six different operating condition cases. Cases 1, 2 and 3 refer to minimum pressure-ratios and Cases 4, 5 and 6 to maximum pressure ratios, at heat-source temperatures of 120, 130 and 140 °C respectively. The results suggest that the expander accounts for the second highest exergy destruction after the evaporator, which agrees well with previous studies [15-17]. The exergy destruction in the condenser is slightly lower than the expander, whilst the exergy destruction in the pump is negligible. At both part and full generator load, an increase in the heat-source temperature results in higher exergy losses, however, these results are normalized by the total, and indicate that at higher pressure ratios and full generator load the losses shift from the evaporator more towards the expander (up to 20-25%, depending on the temperature).

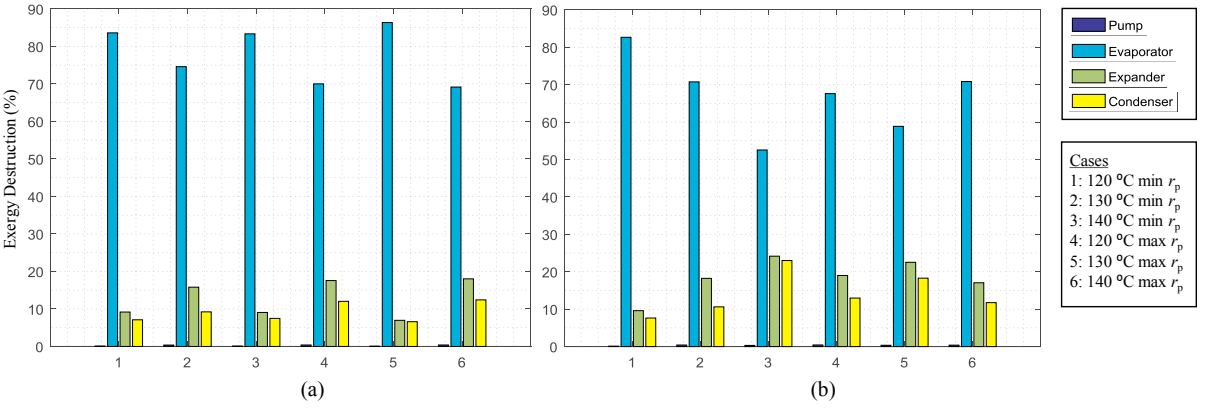

Figure 6: (a) Exergy destruction percentages of different components at different pressure ratios at part generator load. (b) Exergy destruction percentages of different components at different pressure ratios at full generator load.

6. Conclusions

In this paper, we present results obtained from a series of experimental tests on a small-scale (1 kWel) ORC testbed facility, comprising of a rotary-vane pump, a brazed-plate evaporator and a brazed-plate condenser, a scroll expander with a built-in volume ratio of 3.5, and using R245fa as the working fluid. The operating points were varied, resulting in performance characteristics variations that were investigated. Energy and exergy analyses were performed based on the resulting data. Analysis of the experimental results showed that over the range of

investigated heat-source temperatures (120-140 °C), higher pressure ratios led to higher pump power consumptions and higher expander outputs, with expander isentropic efficiencies reaching values up to ~80%. Overall ORC system thermal efficiencies of up to 6% were attained at an intermediate heat-source temperature (130 °C), pressure ratio (3.6) and at full generator load. Both the pump power and expander power, and therefore cycle thermal efficiency were very sensitive to the generator load, but relatively insensitive to the heat-source temperature within the investigated envelope of experimental conditions. An exergy analysis was also performed at chosen operating conditions (minimum/maximum pressure ratios at each heat-source temperature for part/full generator load), and showed that the expander accounted for the second largest exergy destruction after the evaporator.

Acknowledgement

This work was supported by the UK Engineering and Physical Sciences Research Council (EPSRC) [grant number EP/P004709/1]. Data supporting this publication can be obtained on request from cep-lab@imperial.ac.uk.

References

[1] Oyewunmi, O.A., Haslam, A.J. and Markides, C.N. (2015). Towards the computer-aided molecular design of organic Rankine cycle systems with advanced fluid theories. Sustainable Thermal Energy Management Network Conference.
[2] Kirmse, C.J., Oyewunmi, O.A., Haslam, A.J. and Markides, C.N. (2016) Comparison of a novel organic-fluid thermofluidic heat converter and an organic Rankine cycle heat engine. Energies, 9, 479.
[3] Freeman, J., Hellgardt, K., and Markides, C. N. (2015). An assessment of solar-powered organic Rankine cycle systems for combined heating and power in UK domestic applications. Applied Energy, 138, 605–620.
[4] Freeman, J., Hellgardt, K., and Markides, C. N. (2017). Working fluid selection and electrical performance optimisation of a domestic solar-ORC combined heat and power system for year-round operation in the UK. Applied Energy, 186, 291–303.
[5] Markides, C. N. (2013). The role of pumped and waste heat technologies in a high-efficiency sustainable energy future for the UK. Applied Thermal Engineering, 53(2), 197–209.
[6] Vélez, F., Segovia, J. J., Martín, M. C., Antolín, G., Chejne, F., and Quijano, A. (2012). A technical, economical and market review of organic Rankine cycles for the conversion of low-grade heat for power generation. Renewable and Sustainable Energy Reviews, 16(6), 4175–4189.
[7] Cihana E. and Kavasogullari B. (2016). Energy and exergy analysis of a combined refrigeration and waste heat driven organic Rankine cycle system. Thermal Science 2016, (n.d.), 1–12.
[8] Baral, S., Kim, D., Yun, E., & Kim, K. C. (2015). Energy, exergy and performance analysis of small-scale organic Rankine cycle systems for electrical power generation applicable in rural areas of developing countries. Energies, 8(2), 684–713.
[9] Oyewunmi, O. A. and Markides, C. N. (2015). Effect of working-fluid mixtures on organic Rankine cycle systems: Heat transfer and cost analysis. ASME ORC 2015: 3rd International Seminar on ORC Power Systems, 1–10.
[10] Oyewunmi, O.A. and Markides, C.N. (2016) Thermo-economic and heat transfer optimization of working-fluid mixtures in a low-temperature organic Rankine cycle system. Energies, 9, 448.
[11] Imran, M., Usman, M., Park, B., & Lee, D. (2016). Volumetric expanders for low grade heat and waste heat recovery applications. Renewable and Sustainable Energy Reviews, 57, 1090–1109.
[12] Kanoglu, M., Dincer, I. and Rosen, M. A. (2007). Understanding energy and exergy efficiencies for improved energy management in power plants. Energy Policy, 35, 3967–3978.
[13] Mago P.J., Srinivasan K.K., Chamra L.M., and Somayaji C., An examination of exergy destruction in organic Rankine cycles, International Journal of Energy Research, Vol. 32, 2008, 926-938
[14] Aljundi, I. H. (2009). Energy and exergy analysis of a steam power plant in Jordan. Applied Thermal Engineering, 29(2-3), 324–328.
[15] Fatma, C., Kilic, A. and Selman, C. (2016). Energy and exergy analysis of an organic Rankine cycle in a biomass-based forest products manufacturing plant. Turkish Journal of Electrical Engineering & Computer Sciences, 5100–5112.
[16] Kas, Ö. (2014). Energy and exergy analysis of an organic Rankine for power generation from waste heat recovery in steel industry. Energy Conversion and Management, 77, 108–117.
[17] Safarian, S. and Aramoun, F. (2015). Energy and exergy assessments of modified organic Rankine cycles (ORCs). Energy Reports, 1, 1–7.